



# Corrugated interface structure and formation mechanism of Al/Mg/Al laminate rolled by hard plate

Peng-da HUO<sup>1</sup>, Feng LI<sup>1,2,3</sup>, Ye WANG<sup>1</sup>, Chao LI<sup>1</sup>

1. School of Materials Science and Chemical Engineering, Harbin University of Science and Technology, Harbin 150040, China;
2. Key Laboratory of Advanced Manufacturing and Intelligent Technology, Ministry of Education, Harbin University of Science and Technology, Harbin 150080, China;
3. Key Laboratory of Micro-systems and Micro-structures Manufacturing of Ministry of Education, Harbin Institute of Technology, Harbin 150001, China

Received 21 November 2021; accepted 13 April 2022

**Abstract:** A hard plate rolling (HPR) method was proposed to develop the AA1060 Al/AZ31B Mg/AA1060 Al composite plate. The results show that the interface of the traditional Al/Mg/Al composite plate is relatively flat. The hard plate rolling can change the stress state of the composite plate by converting the shear force into compressive stress, and form a differential flow at the Al/Mg interface connection. Consequently, the interface profile becomes corrugated, and the interlaced bond between the layers is achieved. The interfacial bonding strength is 64 MPa, which is four times that of traditionally rolled composite plate. The tensile strength of hard-rolled composite plate can be as high as 210 MPa, which is 12.3% higher than that of the traditional rolling method. In conclusion, the hard plate rolling process provides a new idea for the research of forming and manufacturing high-performance Al/Mg/Al heterogeneous composite plates.

**Key words:** hard plate rolling; Al/Mg/Al composite plate; interface morphology; joint strength; mechanical property

## 1 Introduction

Sustainable development is one of the critical development directions in advanced manufacturing at present. Mg alloy and Al alloy are easy to realize lightweight due to the low density [1–3]. Compared with Mg alloy, Al alloy has higher strength and better corrosion resistance, which is more suitable for industrial application. Compared with Al alloy, the density of Mg alloy is only two thirds of the former, and the weight reduction effect is self-evident. To highlight the embedded benefits of both materials, the combined use of both has become a new trend [4–6]. Due to the difference in melting

point, Mg/Al composite plate can be realized by plastic processes such as extrusion, explosive connection, and rolling.

TANG et al [7] proposed a shunt die co-extrusion process to prepare Al/Mg/Al laminates. The results showed no cavities and cracks at the Al/Mg interface of the composites. The split die design improved the joint strength of the extruded composite plate, but the manufacturing cycle was lengthy and complex.

ZHANG et al [8] prepared Al/Mg composite plates by explosive bonding. The results showed that the diffusion of Mg and Al elements and the formation of intermetallic compounds occurred during annealing. The tensile strength of composite

**Corresponding author:** Feng LI, Tel: +86-451-86392501, E-mail: [fli@hrbust.edu.cn](mailto:fli@hrbust.edu.cn);

Ye WANG, Tel: +86-451-86392501, E-mail: [wangye-2017@126.com](mailto:wangye-2017@126.com)

DOI: 10.1016/S1003-6326(23)66164-3

1003-6326/© 2023 The Nonferrous Metals Society of China. Published by Elsevier Ltd & Science Press

plate first increased and then decreased sharply, and the elongation increased significantly. The fracture mechanism was analyzed by observing crack propagation and interface delamination. Although explosive welding can improve the strength of composite plates, it will cause serious environmental pollution and potential safety hazards.

LUO et al [9] prepared Al/Mg/Al composite plates by hot rolling of two passes. The results showed that the bonding mode of the composite plate was characterized by alternating metal bonding and metallurgical bonding. The intermetallic compound layers,  $Mg_{17}Al_{12}$  and  $Al_3Mg_2$ , could be clearly observed at the connection interface. Through the tensile strength test of the composite plate, the interface was well bonded without any debonding.

In comparison, hot rolling [10,11] is favored because of its low production cost, easy operation, and automation. For the rolled clad plate, the interfacial bonding strength has always been the focus of research [12,13]. Researchers have made many attempts to solve the problem of low interface bonding strength of traditional rolled composite plates. Among them, corrugated roll rolling can achieve the enhanced interface bonding strength [14].

WANG et al [15] prepared Mg/Al composite plates with excellent mechanical properties by rolling with new corrugated roll/flat roll at high temperature. Compared with the discontinuous corrugated interface of explosive welded composite plate by YAN et al [16], WANG et al [15] used a corrugated roll to realize a continuous and

controllable corrugated interface and significantly improve the interface joint strength. However, it was necessary to add the pre-fabrication process of the corrugated interface on one side of the plate first, and then the rolling of the composite plate was conducted.

If the stress state of the clad plate is changed, the interface morphology and joint strength will also change. Therefore, a new clad plate rolling method is proposed in this work. In the conventional rolling of composite laminates, there is rolling friction between the roll and the slab. In traditional rolling of composite laminates, there is rolling friction between rolls and plates. After adding the hard plate, the rolling force is transferred to the composite plate through the hard plate. The friction between hard plate and composite slab becomes sliding friction. The change of stress state has a great influence on the bonding strength, interface morphology, contour characteristics and microstructure of the composite plate.

## 2 Experimental

### 2.1 Process principle

The joint strength of the composite plate is one of the critical indexes to evaluate the plate. Adding the hard plate between the roller and the composite plate changed the friction condition at the interface and the deformation behavior of the composite plate. The change of stress state inevitably affected the strength and performance of the composite plate. The process principle comparison between hard plate rolling and the traditional rolling composite plate is shown in Fig. 1.

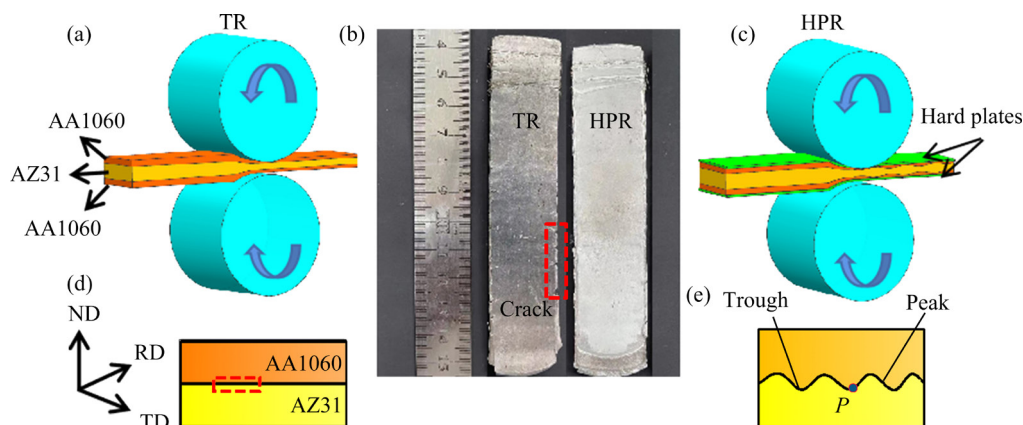


**Fig. 1** Rolling process principle: (a) Traditional rolling (TR); (b) Physical comparison; (c) Hard plate rolling (HPR); (d) Interface morphology of traditionally rolled sample; (e) Interface morphology of hard plate rolled sample (ND–Normal direction; RD–Rolling direction; TD–Transverse direction)

The large deformation rolling can be realized on hard plate [17]. According to the existing research, the optimal reduction of the hard plate rolling composite plate was about 60% [18]. To facilitate comparison with traditional rolling, the purpose of this study was to study the rolling of composite plate with and without hard plate where the total reduction was 55%. Because there was no support of hard plate in traditional rolling, the reduction of single-pass should not be too large [19]. Under the condition of keeping the total reduction unchanged, experiment of traditional rolling was adjusted to three-pass rolling (30%+20%+20%). Figure 1(b) shows the physical figures of the composite plate obtained by traditional rolling and hard plate rolling. Due to the large cumulative deformation in traditional rolling, the composite plate has the characteristics of edge crack and slight bending. In contrast, the composite plate has no bending and edge crack after hard plate rolling. Figures 1(d, e) show the schematic diagrams of the interface connection morphology for the composite plate by traditional rolling and hard plate rolling. The interface morphology of the connection part of the hard plate rolling clad plate changes from linear to wavy connection. In order to facilitate in-depth analysis, the characteristic features of the wavy connection interface are named peak and trough, respectively [20].

## 2.2 Research program

Commercial rolled AZ31B Mg alloy and AA1060 Al alloy plate were used as experimental raw materials, and their compositions are given in Table 1.

**Table 1** Compositions of AZ31B Mg alloy and AA1060 Al alloy (wt.%)

Material	Mg	Al	Mn	Cu	Fe	Zn	Ca
AZ31B	95.45	3.9	0.334	0.05	0.005	0.81	0.04
AA1060	0.03	99.6	0.03	0.05	0.35	0.05	–

Mg plate with a thickness of 5 mm, Al plate with a thickness of 0.5 mm, and hard plate with a thickness of 1 mm were prepared for the test. The Mg/Al plate was machined to the same size, i.e. length ( $L$ ) of 6 mm and width ( $d$ ) of 3 mm. The slab was pretreated before rolling. Firstly, the surfaces of Mg and Al plates were polished with coarse

sandpaper, and then soaked in acetone solution to remove impurities such as oil on the surface. The surface of the plate was cleaned with alcohol and dried naturally. A layer of high-temperature isolating agent (boron nitride) was sprayed on the inner surface of the hard plate to prevent the Al plate and the hard plate from bonding together during hot rolling. The composite plates required by the traditional rolling (TR) process were stacked in the order of Al/Mg/Al and fixed with iron wire. For hard plate rolling, a hard plate was connected to the surfaces of the Al/Mg/Al composite plate, as shown in Fig. 1(c). The same fixing method was used to combine the composite plate with the hard plate. The fixed composite plate was preheated at 300 °C for 0.5 h. After preheating, the fixed end of the hard plate was sent to the rolling mill for rolling. The rolled composite plate was annealed at 300 °C. The rolling angular speed was 6 rad/s and the rolling temperature was 350 °C.

## 2.3 Microstructure and property characterization

The scanning electron microscope (SEM) equipped with an energy dispersive spectrometer (EDS) was used to characterize the interface morphology of traditional rolling and hard plate rolling composite plate (RD–ND). Optical microscopy (OM), SEM, and electron backscattered scattering detection (EBSD) were used to characterize the microstructure and the existence of intermetallic compounds in matrix Mg. EBSD samples were polished on sandpaper and then mechanically polished. The burrs on the metal surface were removed by electrolytic polishing. Phosphoric acid and ethanol were selected as the polishing solutions with current of 0.3 and 0.2 A, respectively. In order to achieve the best effect, the total polishing time was 150 s. The tilt of the test bench was 70°. The working distance was 12 mm, and the scanning step was 1.5 μm. The scanning area of EBSD was 200 μm × 200 μm. Channel 5.0 software was used for analysis. The test was carried out under the X'pert Pro X-ray diffractometer. The tube voltage was 40 kV, and the tube current was 40 mA. The bonding area on the side of Al/Mg/Al was scanned continuously. The scanning range was 20°–80°, and the scanning speed was 1 (°)/s. The tensile test specimens of the original Mg plate, Al plate, traditionally rolled composite plate, and hard rolled composite plate were tested by using the

Instron 5569 material testing machine. Each tensile sample was taken from the center of the plate, and multiple experiments were carried out to eliminate errors. The tensile rate was 1 mm/min. The tensile test was referred to ASTM E8/E8M—2013a. The tensile shear strength test was carried out along the rolling direction (RD) at room temperature.

### 3 Results and discussion

#### 3.1 Interface morphology

The interface morphology and structural characteristics of the connection part of the composite plate determine the joint strength and performance. When the reduction is 55%, the comparison results of interface morphology of composite plate under the conditions of traditional rolling and hard plate rolling are presented in Fig. 2.

Figure 2(d) shows the interface structure of the Al/Mg/Al composite plate obtained by traditional hot rolling. It can be seen that the interface contour of the joint is clear, smooth, and almost linear as a

whole. As shown in Fig. 2(b), although the outline of the bonding interface fluctuates slightly, the amplitude is small and can be ignored. As shown in Fig. 2(a), there are holes at the visual interface [21]. Under annealing condition, there is a transparent transition layer at the interface, indicating the metallurgical bonding [22], as shown in Fig. 2(c). The bonding area between the interfaces of traditionally hot-rolled composite plates is small. The interface morphology of the hot-rolled Al/Mg/Al composite plate after adding the hard plate is shown in Fig. 2(h). It can be seen that the Al/Mg bonding interface on one side of the composite plate is regularly wavy, without defects such as holes and cracks. More importantly, the interface has good bonding quality. To further explore the interface morphology and structural characteristics of the composite plate after a single-pass rolling, a hard and brittle intermetallic compound (IMC) layer is formed at the Mg/Al interface after annealing at 300 °C. According to the film theory [23], the brittle layer at the interface to

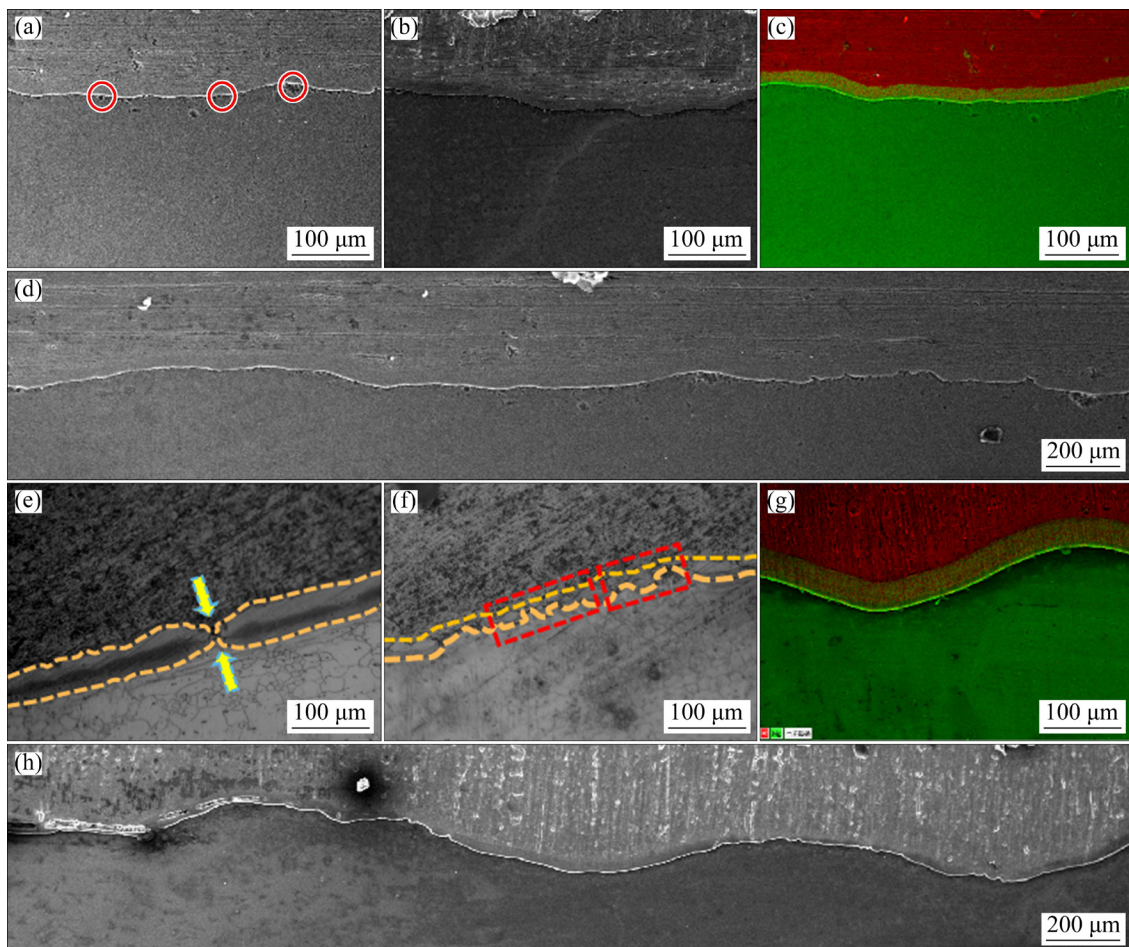


**Fig. 2** Comparison of interface morphology between traditionally rolled and hard plate rolled Al/Mg/Al composite plate: (a–d) Traditional rolling; (e–h) Hard plate rolling

be bonded will be broken under the action of rolling force during deformation, exposing fresh metal to achieve metallurgical bonding. Figure 2(e) is a partial magnification of the interface close to the trough of Fig. 2(h). In Fig. 2, it can be seen at the arrow mark where the rolling is carried out after adding the hard plate, the primary fresh matrix Mg and cladding Al metal break through the oxide layer and are squeezed into the intermetallic compound. The metals Al and Mg are conically pinned at the upper and lower positions of the joint surface. This mechanical locking method can improve the interface bonding quality [24]. Figure 2(f) shows the interface morphology at the waist of the ripple. It can be seen that some intermetallic compounds at the interface are broken. The shape of a wall by the mutual engagement between the Mg and Al plates makes the interface locked and increases the connection force [25]. Figure 2(g) shows a surface scanning view of a complete wavy connection part at the connection interface. It can be seen that there are a large number of Al and Mg elements at the bonding interface, indicating that the composite plate has achieved metallurgical bonding. The corrugated interface similar to sinusoidal curve is continuous and flat. The peak is 65  $\mu\text{m}$ . Intermetallic compounds are continuously and evenly distributed. The two metals squeeze each other to form regular bulges and depressions at the interface.

The finite element simulation of advanced plastic forming is used to analyze the reason why the interface of hard plate rolling composite plate presents wavy morphology. The displacement change and effective strain can be observed at the

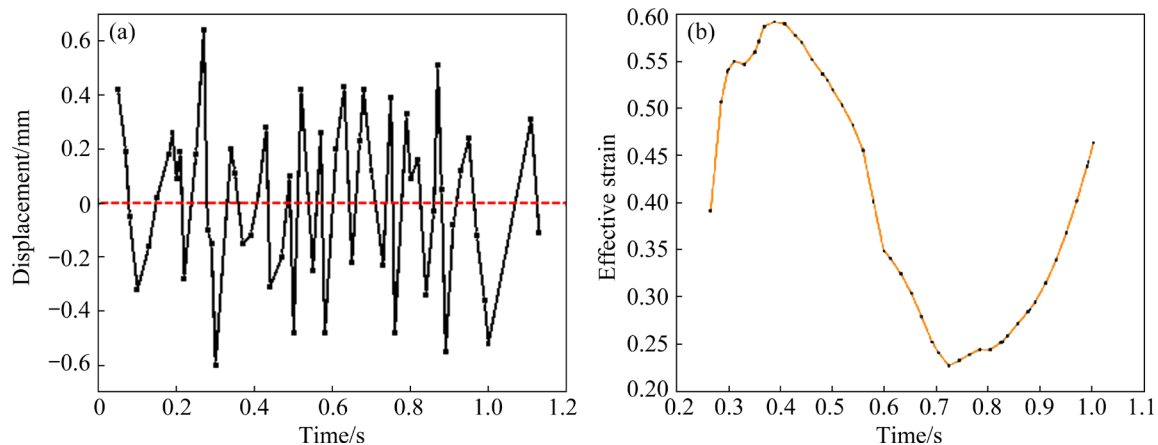
typical position at the Mg/Al interface, as shown in Fig. 3. The point location is shown at Point *P* in Fig. 1(e).

Figure 3(a) shows the displacement change of the metal at the interface. With the progress of rolling, the displacement fluctuates regularly up and down. The simulation shows that Al/Mg plates are in a state of mutual bite at the bonding interface. Figure 3(b) shows the effective strain at Point *P* in a complete cycle along the RD. It can be seen that a continuous curve appears in the whole fluctuation cycle. The effective strain at the peak can reach 0.59, and the maximum difference between the peak and trough of the curve is 0.385.

### 3.2 EDS results

Because the Al/Mg/Al composite laminate is geometrically symmetric from top to bottom, only one side is sampled for analysis. Figure 4 shows the comparison of the interface morphology of the composite plate rolled with and without hard plate after annealing at 300  $^{\circ}\text{C}$ .

It can be seen from the interface morphology in Fig. 4 that the diffusion layer at the interface of traditional rolling without a hard plate is not apparent. In contrast, the diffusion layer can be clearly observed during hard plate rolling, and the interface is closely connected. According to the EDS results, the thickness of the interface diffusion layer of the hard plate rolled composite plate can reach 32  $\mu\text{m}$ . It can be seen from Fig. 4 that the IMC consists of two layers,  $\text{Mg}_{17}\text{Al}_{12}$  near the Mg side and  $\text{Mg}_2\text{Al}_3$  near the Al side [26]. According to the existing research [27], Al diffuses to the close contact layer faster than Mg, so the thickness of the



**Fig. 3** Finite element simulation of hard plate rolling: (a) Metal displacement curve at interface; (b) Effective strain curve at typical point

$Mg_2Al_3$  layer is larger than that of the  $Mg_{17}Al_{12}$  layer. In comparison, the IMC thickness of hard plate rolling is slightly larger than that of traditional rolling.

### 3.3 Phase composition

To further determine the composition of the IMC phase at the interface during rolling with and without hard plate, the composite plate was stripped along the Al/Mg interface to expose the IMC layer, and its composition was analyzed by XRD. Figure 5 shows the phase composition of Mg and Al sides of the tear surface of a rolled composite plate with and without the hard plate, respectively.

In Fig. 5(a), there are  $Mg_{17}Al_{12}$  and  $Mg_2Al_3$  intermetallic compounds at the interface of rolling with and without hard plate. However, it can be seen from the comparison of local magnifications

that there are more  $Mg_2Al_3$  peaks in the hard plate rolling. At the same time, it is found that there are multiple peaks of Al on the Mg stripping surface of hard plate rolling. Compared with the rolling without hard plate, Al is not detected on the Mg side, and the existence of Al on the Mg surface of the hard plate also indirectly indicates that the bonding strength of the hard plate rolled composite plate is higher. In Fig. 5(b), it is observed that  $Mg_{17}Al_{12}$  and  $Mg_2Al_3$  intermetallic compounds also exist on the Al side of the interface, which indicates that metallurgical bonding can be achieved under the conditions of traditional rolling and hard plate rolling [25].

### 3.4 Microstructure of Mg matrix

As can be seen from Fig. 6, there is a large number of dynamic recrystallization and twinning

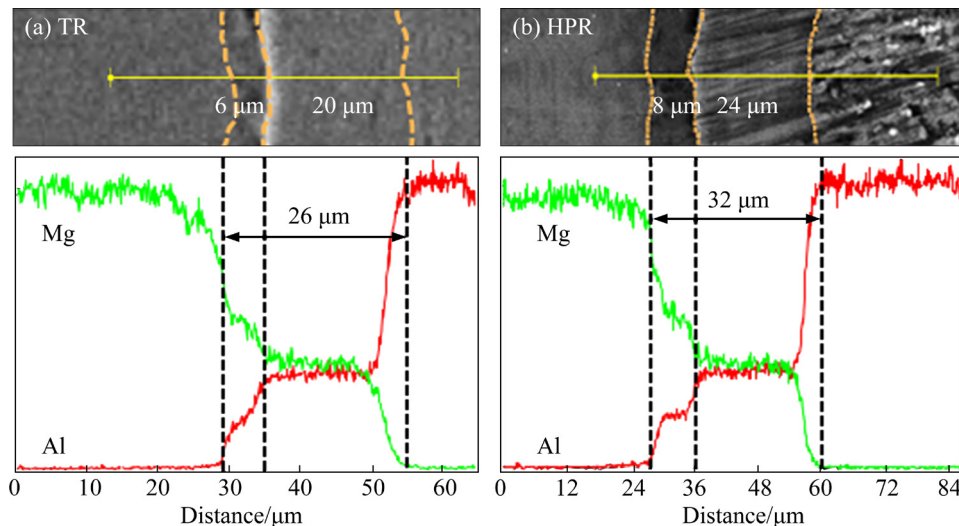


Fig. 4 Microstructure and EDS results of Al/Mg/Al unilateral interface: (a) Without hard plate; (b) With hard plate

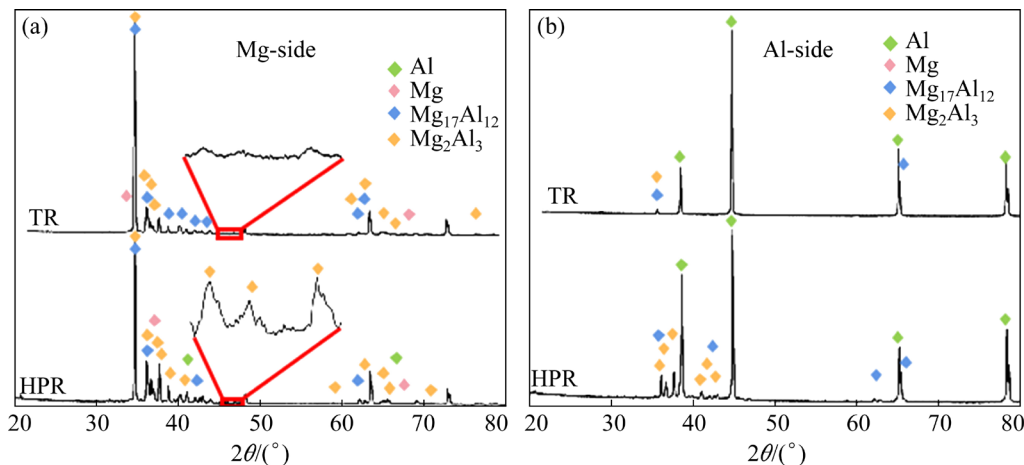
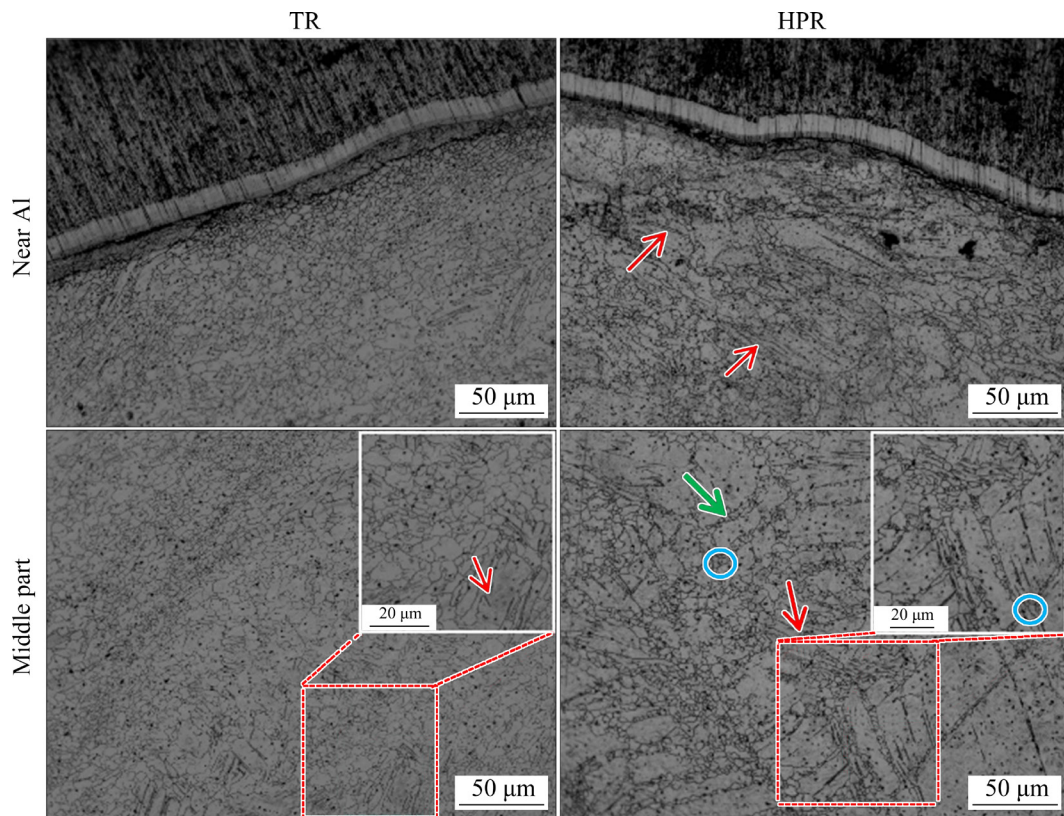


Fig. 5 XRD patterns on tear surface of rolled composite plate with and without hard plate: (a) On Mg side; (b) On Al side



**Fig. 6** Comparison of microstructures in Mg plate under different conditions

in the traditionally rolled and hard plate rolled composite plate. Figure 6(a) shows the metallographic structure of the Mg plate at the Al/Mg interface of traditional rolling. It is found that the grains are gradually refined near the side of Al plate. As can be seen from Fig. 6(b), there are many twins with lamellar structure in the structure of the Mg plate, in the form of parallel twins. For the middle frame of the Mg plate, the matrix structure of the traditionally rolled Mg plate is shown in Fig. 6(c). It can be seen that some parallel twins are formed at the edge, mainly in larger grains. It is reported [28] that the parallel-twin region usually has low energy storage, so DRX is difficult to occur. The Mg matrix structure of hard plate rolled plate is shown in Fig. 6(d), and there are both parallel and cross twins. Cross twinning (blue circle position) accounts for the central part, and most of the cross twinning angles are close to vertical. In Fig. 6(d), it is easy to see that most twins have recrystallized, and only a few twins have not recrystallized, maintaining the lamellar structure (red arrow). Most of the recrystallized grains are gathered together and distributed in the shape of rectangular. Some recrystallized grains still gather together in a strip

shape and retain the twin interface morphology (green arrow). The recrystallized grains aggregated into blocks are mainly mixed between strip twins. The recrystallization in the strip cuts the original twin grain into several parts. Due to the limitation of the twin size, the recrystallized grains nucleate in the original grain boundary of the twin. The recrystallized grain size which is not affected by twin size is larger.

To further explore the recrystallization changes in two processes, the recrystallization of the Mg plate was analyzed by EBSD. Figures 7(a, b) show the recrystallized EBSD in the Mg matrix with and without hard plate, respectively. Figure 7 shows that fine-equiaxed grains and commonly-grown recrystallized grains caused by annealing after rolling exist in both processes. Most of the recrystallized grains in traditional rolling are equiaxed grains, while the recrystallized grains in hard plate rolling show a long strip shape and grow more orderly along the RD. In particular, the fraction of recrystallized grains in the microstructure of Mg plate rolled by hard plate significantly increases to 46%, which is 6% higher than that of the traditional rolling (Fig. 7(d)). The

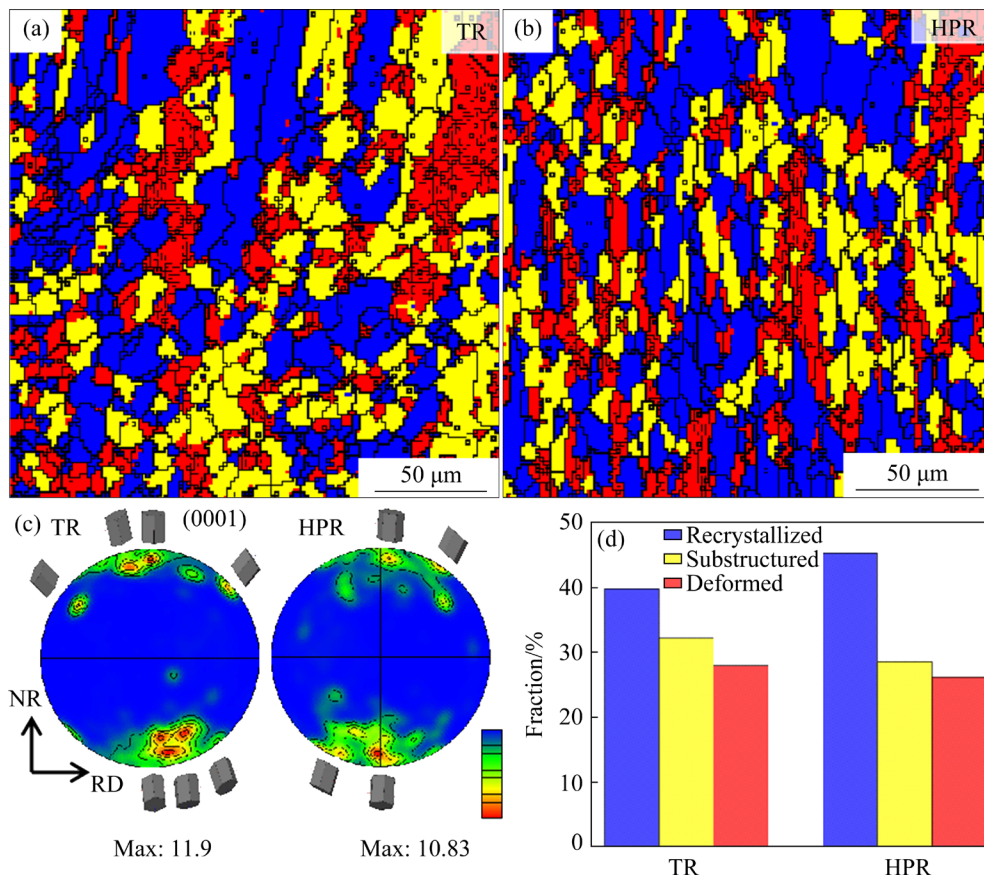


**Fig. 7** Recrystallization structure of rolled composite plate with or without hard plate: (a) Traditional rolling; (b) Hard plate rolling; (c) Recrystallization pole figure; (d) Percentage of grain types

low-angle grains are relatively few, which indicates that the recrystallization is more sufficient under the rolling of hard plate. Figure 7(c) shows the recrystallization {0001} pole figure of traditional rolling and hard plate rolling, respectively. It can be seen that the  $c$ -axis of the grains is relatively evenly distributed around the deviation of the ND by  $7^{\circ}$ – $18^{\circ}$ . The peak points show multi-point distribution, which are not strictly in the ND. Compared with traditional rolling, the recrystallization texture strength of hard plate rolling decreases. The maximum pole density is 10.83.

### 3.5 Joint strength

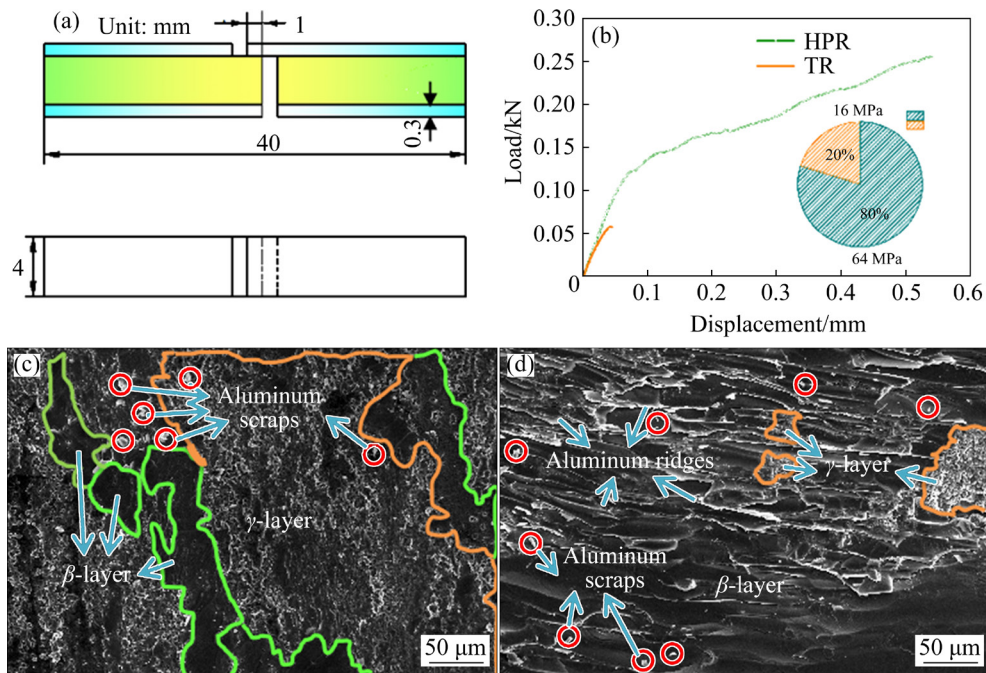
To evaluate the joint strength at the interface of the composite plate, the shear strength of the sample is tested. The results and the fracture morphology are shown in Fig. 8.

Figure 8(a) shows the dimensions of the specimen for testing shear strength. The specimens were prepared by cutting along the RD at the center of each rolled plate. Figure 8(b) shows the load–

displacement curves of the samples rolled with and without the hard plate. The calculation formula [29] of shear strength ( $\tau$ ) is

$$\tau = F/A \quad (1)$$

where  $F$  stands for shear force;  $A$  represents the area of Al/Mg contact surface. Figure 8 shows that the interface of the composite plate prepared by traditional rolling breaks within the tensile distance of less than 0.1 mm. The plate prepared by hard plate rolling leaves at the tensile length of 0.55 mm, and the tensile shear strength can reach 0.256 kN. According to the formula calculation, the interfacial shear strength of the composite plate can be obtained. As shown in Fig. 8(b), the interfacial shear strength of Al/Mg/Al composite plate obtained by hard plate rolling can reach 64 MPa, which is four times that of traditional rolling. Figures 8(c, d) show the fracture morphologies of the Mg side after shear tension of traditionally rolled and hard plate rolled composite plates. Due to the insufficient bonding force of the traditional rolling interface (Fig. 8(c)), the discontinuity is



**Fig. 8** Interface shear strength test results: (a) Shear strength test sample size; (b) Load–displacement curves of plates rolled with and without hard plate; (c) Tensile fracture morphology of Mg side in traditional rolling; (d) Tensile fracture morphology of Mg side in hard plate rolling

stripped in-plane mode [30]. The fracture is composed of large area  $\gamma$  layer ( $\text{Mg}_{17}\text{Al}_{12}$ ) and strip  $\beta$  layer ( $\text{Mg}_2\text{Al}_3$ ). Small amounts of Al chips adhere in the layer. However, the fracture tearing on the magnesium side of hard plate rolling is obvious. The fracture presents zigzag flow and forms stepped morphology. It is mainly composed of  $\beta$  layer. Many Al ridges (bright stripes in Fig. 8(d)) are arranged alternately at the fracture, and the number of Al chips is also relatively increased. XRD pattern also verifies the existence of Al on the Mg fracture surface. The crack which is produced by traditional rolling only passes through the hard brittle phase,  $\gamma$  layer and  $\beta$  layer, by plane mode. The cracks in the samples rolled by hard plate pass through  $\beta$  layer by zigzag shape and leave a lot of Al chips on the ridge. The different fracture modes indicate that the more intense the crack propagation, the more the energy is required. From the change of fracture mode, the evolution law of interfacial bonding strength can be inferred.

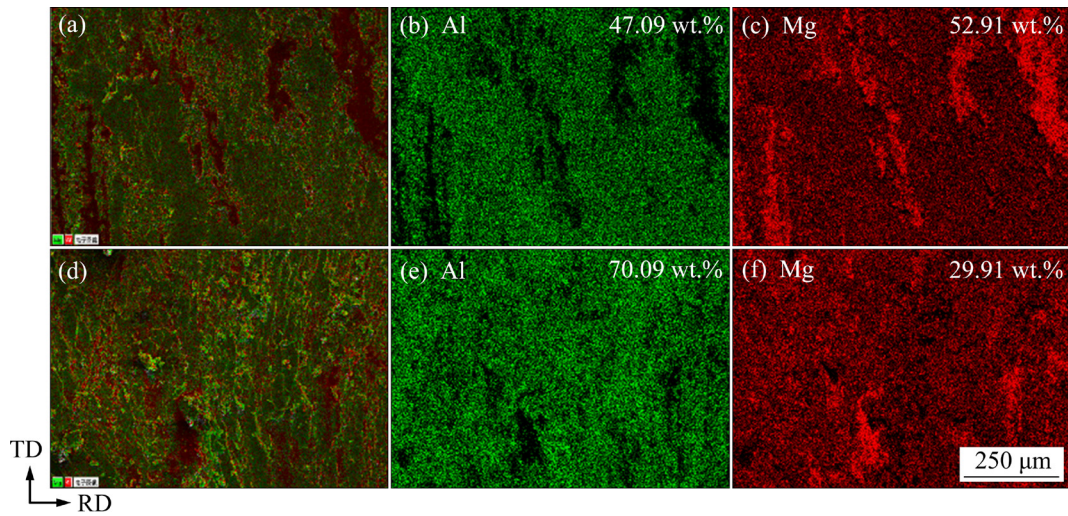
Figure 9 shows the fracture morphology characteristics and element distribution on the Al side of the composite plate. According to the elemental analysis of surface scanning, the contents of Al and Mg in traditional rolling are 47.09% and 52.91%, respectively, and the ratio of Al to Mg is

close to 1:1. The ratio of Al to Mg in the fracture surface of the hard plate rolling is 7:3. It is inferred from the ratio that the compound at the interface is closer to  $\text{Mg}_2\text{Al}_3$ . It is indirectly confirmed that the tensile fracture microstructure of the rolled plate without hard plate mentioned above is composed of  $\text{Mg}_{17}\text{Al}_{12}$  and  $\text{Mg}_2\text{Al}_3$  [31], while that of the rolled plate with hard plate is mainly composed of  $\text{Mg}_2\text{Al}_3$ . The comparison shows that distribution of fracture interface elements is more uniform after hard plate rolling. It can be known from Fig. 9(d) that compared with the interface fracture morphology on the Mg matrix side in Fig. 8(d), the stepped feature of the fracture morphology on the Al matrix side becomes gentle. Due to the uneven stress of wave peaks and troughs at the interface [20], Mg is mainly distributed on the Al ridge.

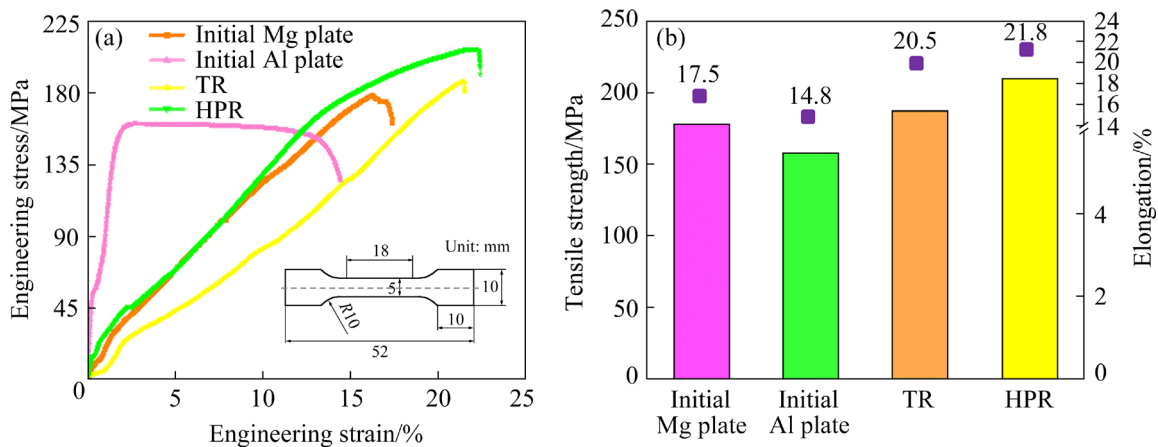
### 3.6 Mechanical property

Figure 10 shows the mechanical properties of rolled composite plates with and without the hard plate through the tensile test.

As shown in Fig. 10(a), compared with traditional rolling, the tensile strength and elongation of the composite plate after hard plate rolling are improved to varying degrees. The tensile



**Fig. 9** Element distributions of tensile shear fracture surface of Al side: (a–c) Traditional rolling; (d–f) Hard plate rolling



**Fig. 10** Engineering stress–engineering strain curves (a) and mechanical properties (b)

strengths of the raw Mg and Al slabs are 178.2 and 157.3 MPa, respectively. After traditional rolling, the tensile strength of the composite plate is improved to be 187 MPa, and the total elongation at fracture ( $A_t$ ) reaches 20.5%. Due to the change of the interface bonding strength and the structure of the matrix Mg plate, the overall mechanical properties of the hard plate rolled composite plate are better. The tensile strength is increased from 187 to 210 MPa, with an increase of 12.3%, and the  $A_t$  is increased to 21.8%.

### 3.7 Fracture morphology

Figure 11 shows the comparison of tensile fracture morphology of rolled composite plates with and without hard plate.

It can be seen from Fig. 11(a) that the

traditionally rolled Mg/Al section is relatively flat. The fracture surface of the matrix is smooth. The Mg plate and Al plate are completely separated. Figure 11(b) shows that the fracture of Mg plate and Al plate rolled by hard plate is serrated and keeps a close bonding state. Compared with traditional rolling, the fracture of matrix Mg plate in hard plate rolling is generally divided into two parts. One is the matrix Mg near the bonding interface. Due to its microstructure and interface bonding strength, the fracture morphology characteristics change from smooth to rougher, and the increase of surface roughness and the enhancement of interface bonding ability complement each other. Second, the middle part of the Mg plate is similar to that of the traditional rolling fracture, resulting in brittle fracture and ductile fracture. However, the

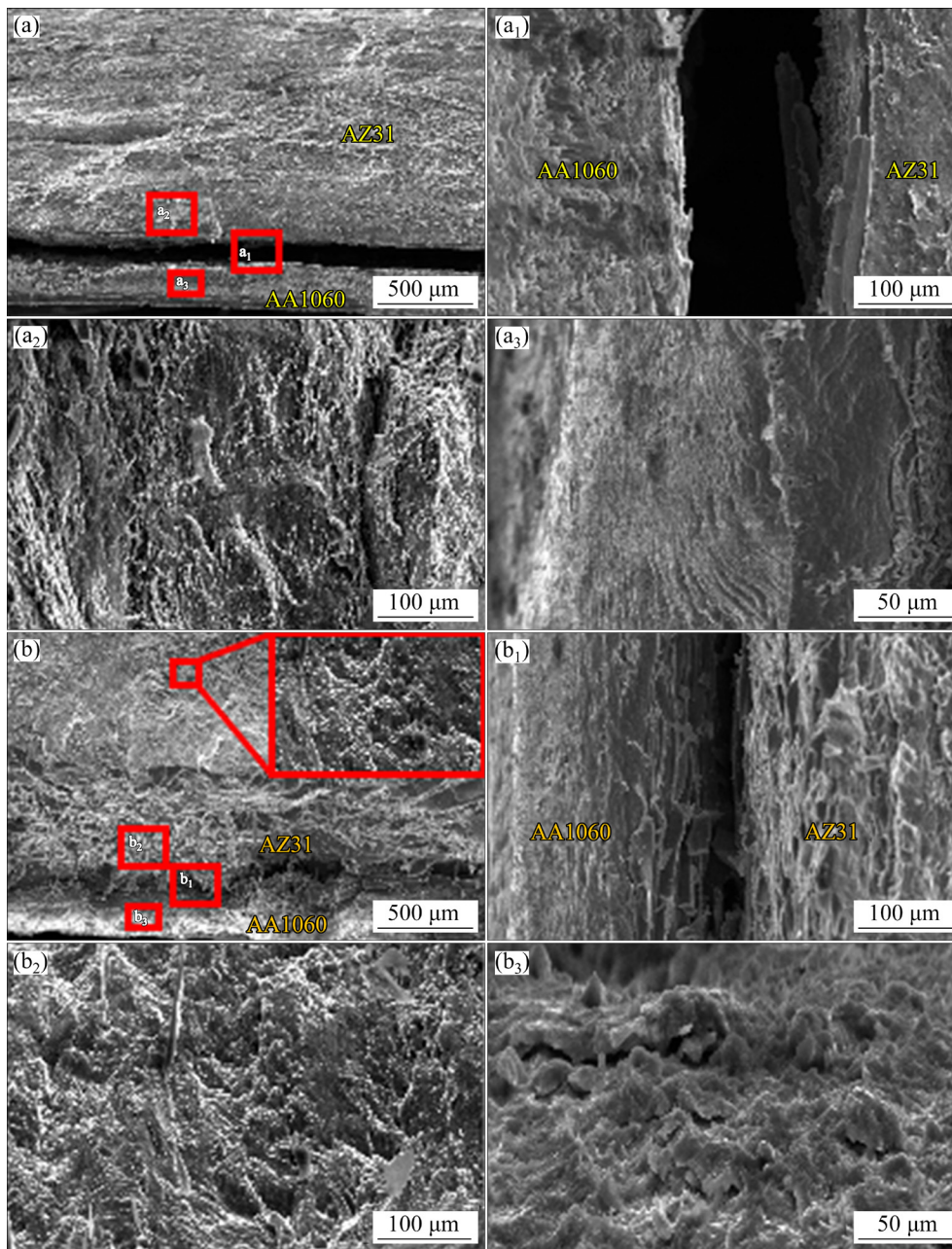


**Fig. 11** Fracture morphologies of traditionally rolled (a) and hard plate rolled (b) composite plates: (a<sub>1</sub>, b<sub>1</sub>) Mg/Al joint; (a<sub>2</sub>, b<sub>2</sub>) Matrix Mg; (a<sub>3</sub>, b<sub>3</sub>) Cladding Al

differences are that there are many dimples at the fracture of Mg matrix rolled by hard plate, mainly exhibiting ductile fracture. It is known from Figs. 11(a<sub>3</sub>, b<sub>2</sub>) that AA1060 has good ductility and obvious necking phenomenon. The fracture on Al side presents cleavage fracture mode with obvious river pattern. Compared with traditional rolling, there are unique characteristics on the fracture surface of Al plate rolled by hard plate, as shown in Fig. 11(b<sub>3</sub>). In addition to dimples, microcracks appear on the Al matrix, induced by high bonding strength.

## 4 Discussion

### 4.1 Generation and characteristics of corrugated interface

Because the composite plate is in direct contact with the roll in traditional rolling, the stress is more uniform. Therefore, unlined plate interface in Fig. 2 is relatively straightforward. The hard plate can transform the traditional rolling friction into sliding friction, which dramatically changes the stress state during forming. It is

particularly stressed that in traditional rolling, shear deformation is the main way in which the plastic sheet is deformed. The hard plate can convert the shear stress of the roll into compressive stress. In comparison to traditional rolling, the shear stress of rolled plates clamped by the hard plate decreases and the compression stress increases. At the same time, the increase of the compressive stress of the Al plate in direct contact with the rolled plate results in the change of the flow direction. The different stress causes the uneven flow of two metal plates at the interface. Finally, the flow pattern shown in Fig. 3(a) is formed with the help of the hard plate, and the Al and Mg are extruded with each other along the RD to finally form a corrugated interface.

Due to the large reduction selected for hard plate rolling, cracks appear at the plate connection interface under the strong shear stress of the roll. The hard plate can reduce the shear stress and add compressive stress to fill the metal Al and Mg in the crack. While inhibiting crack growth, special interface structures such as Figs. 2(e, f) appear locally. This “pinning” and “Great Wall” connection mode is consistent with the corrugated interface

in structure, realizes mechanical interlocking, and significantly enhances the interface connection performance.

### 4.2 Deformation mechanism

#### 4.2.1 Influence of interface morphology on shear-tensile properties

Figure 12 shows the effect of different interface morphologies of composite plate on tensile and shear properties. In Fig. 12, the finite element analysis software ANSYS is used to study the maximum shear stress at the flat interface of traditionally rolled composite plate and the corrugated interface of hard plate rolling in the process of shear and tension. According to the above experimental data, the maximum strength of interfacial welding force is preliminarily set as 64 MPa. As shown in Fig. 12, when the tensile force of the flat interface under traditional rolling is 500 N, the fatigue limit of the material can be reached at the edge of the bonding interface, while the tensile force of the corrugated interface of hard plate rolling needs to get 2000 N. This shows that under the same fatigue strength, the corrugated interface produced by the hard plate rolling can

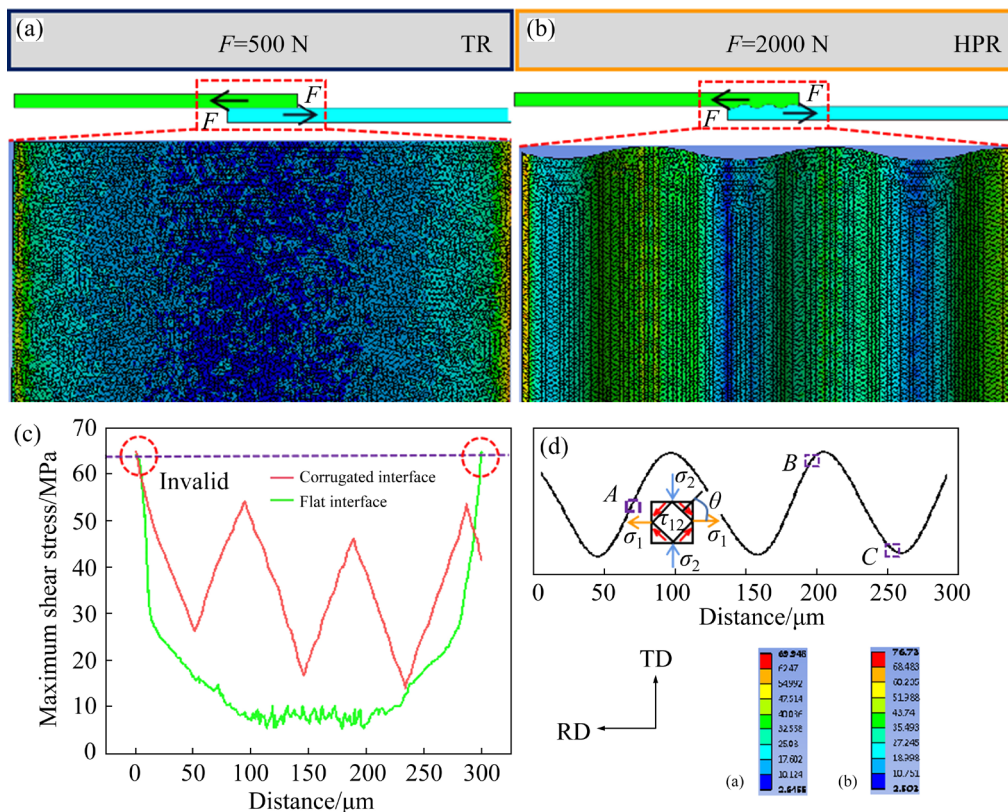


**Fig. 12** Numerical simulation of shear tension: (a) Traditional rolling flat interface; (b) Hard plate rolling corrugation interface; (c) Maximum shear stress curve; (d) Pure shear stress analysis of corrugated interface

effectively improve tensile strength. Figure 12(c) shows that the critical shear stress of the two bonding interfaces occurs at the geometric edge. However, there is a great difference between the low stress zone and the high stress zone at the flat interface formed without hard plate rolling. The comparison shows that the flat interface is easy to produce stress concentration in the process of shear and tension. The stress concentration at the geometric edge allows the material to achieve its fatigue strength in advance, leading to fatigue cracks, and then the laminated material begins to peel off. The maximum shear stress distribution at the corrugated interface is more uniform, so that the transition of the stress from the low-stress area to the high-stress area tends to be gentle. Figure 12(d) shows the pure shear stress analysis of wave peak, wave trough, and hillside of the corrugated interface during shear tension. The shear stress at the interface (*A*) is the tangential component of the tensile stress. The shear stress near the wave peak (*B*) and the wave trough (*C*) increases and changes with  $\theta$ . Therefore, the corrugated structure can significantly weaken the shear stress of the interface under the same tensile stress.

#### 4.2.2 Shear–tensile fracture mechanism

According to the above shear–tensile test results and XRD analyses, the fracture modes of rolling composite plate with and without hard plate

near the interface of heterogeneous laminates are different. Therefore, in order to further explore the fracture mechanism at the interface, Fig. 13 shows the fracture section and mechanism diagram. Figures 13(a, b) show the metallographic images of the fractured material at the Al/Mg interface (RD–ND) with and without hard plate rolling, respectively. Figures 13(c, d) show the corresponding fracture mode and mechanism.

Figure 13(a) shows that the crack at the fracture originates from the IMC and only extends in  $\beta$  layer and  $\gamma$  layer. Compared with traditional rolling, the crack of hard plate rolling also starts from the brittle layer, but its propagation is stronger. The crack mainly propagates in  $\beta$  layer and terminates in Al layer. This is also the reason for many Al ridges in hard plate rolling fracture in Fig. 7. For the rolling of Al/Mg/Al composite plate, the metallurgical bonding area generated by active atom diffusion can increase the interfacial bonding strength. Still it inevitably occurs in the brittle interfacial reaction layer during the fracture process, to reduce the interfacial bonding strength [31]. However, compared to the traditional rolling fracture in the IMC layer, the hard plate rolling due to the wave interface enhances the interfacial bonding force, and the fracture occurs mainly in the  $\beta$  layer or even in the Al layer.

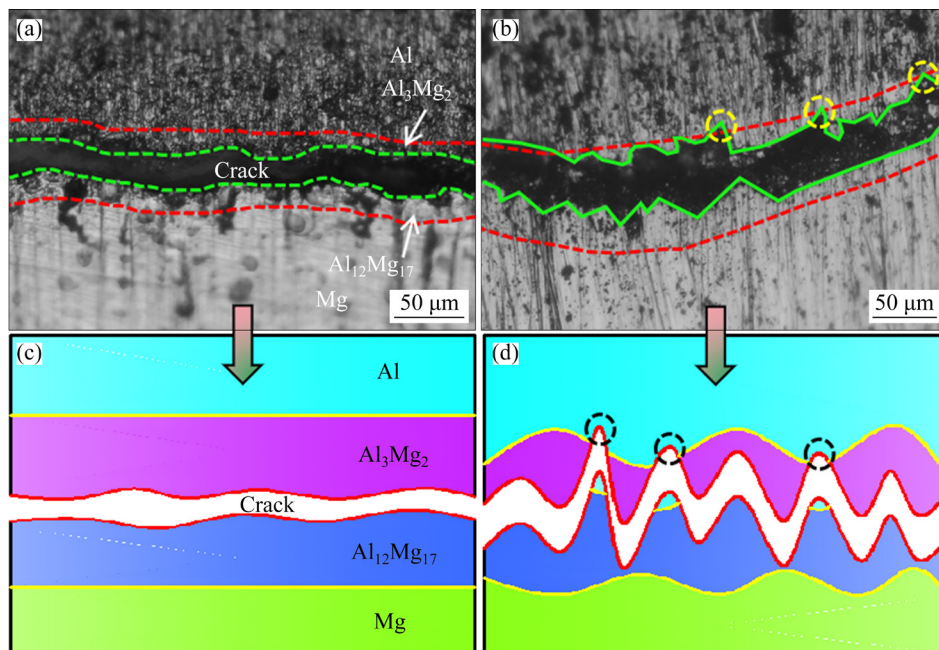


**Fig. 13** Schematic diagram of fracture mode and mechanism of Al/Mg interface: (a, c) Traditional rolling; (b, d) Hard plate rolling

### 4.3 Recrystallization structure in Mg plate

Because the single-pass reduction selected for hard plate rolling is large. For the Mg plate, its close hexagonal structure makes the slip not meet the demand under large deformation. At this time, the twins generated in the Mg matrix coordinate the plastic deformation. As shown in Fig. 6, compared with the traditional rolling with small deformation, the cross twins generated in hard plate rolling have higher storage energy, which is helpful to refining the matrix grains and serves as the preferred nucleation position for dynamic recrystallization. In addition to the effect of twinning, the composite plate can reduce the heat loss during rolling under the protection of hard plate, which also promotes dynamic recrystallization during the plastic deformation. The above reasons also clarify the increase of recrystallization in Mg plate under hard plate rolling in Fig. 7(d). It can be seen from Fig. 7(c) that the texture is weakened with the increase of recrystallization during hard plate rolling. The residual stress in the rolled composite plate is reduced and the tensile properties of the plate are significantly improved.

## 5 Conclusions

(1) The interface profile of the Al/Mg/Al composite plate obtained by traditional hot rolling is flat. The addition of hard plate can change the stress state of composite plate in the rolling process and make the interface profile show wavy regular characteristics. The corrugated interface can realize the interlocking between composite plates and significantly improve the bonding strength. And there are no pores, impurities, and other defects at the interface. At the same time, twin activation in Mg alloy matrix promotes recrystallization and grain refinement.

(2) Hard plate rolling can transform shear stress into compressive stress. The uneven metal flow formed at the plate interface promotes the fresh metal to penetrate the oxide layer and increase the contact area, which makes the metallurgical bonding more complete. Under the same rolling conditions (temperature and reduction), the IMC thickness of composite plate prepared by hard plate rolling is larger than that of traditionally rolled composite plate. The wavy bonding mode can increase the area of IMC layer and interface

welding force, and make the bonding between heterogeneous composite plates more firm.

(3) The interfacial bonding strength of the Al/Mg/Al composite plate prepared by hard plate rolling was tested by the tensile–shear test. The results show that the interfacial bonding strength is 64 MPa, which is four times that of traditional hot rolling. The shape quality of the composite plate obtained by hard plate rolling is good, and the comprehensive properties are significantly improved. The tensile strength is 210 MPa, and the total elongation at fracture is 21.8%. Therefore, the hard plate rolling can significantly improve the mechanical properties of the composite plate, due to the corrugated interface and matrix structure of the plate.

## Acknowledgments

This work was supported by the Natural Science Foundation of Heilongjiang Province, China (No. JQ2022E004).

## References

- [1] WANG Yang, ZHANG Shun, WU Rui-zhi, TURAKHODJAEV N, HOU Le-gan, ZHANG Jing-huai, BETSOFEN S. Coarsening kinetics and strengthening mechanisms of core–shell nanoscale precipitates in Al–Li–Yb–Er–Sc–Zr alloy [J]. *Journal of Materials Science & Technology*, 2021, 61: 197–203.
- [2] HE Ying-jie, XU Hong-yu, HU Mao-liang, JIANG Bo, JI Ze-sheng. Effect of glucose concentrations on wear resistance of Al/APC composites prepared by hydrothermal carbonized deposition on chips [J]. *Journal of Materials Science & Technology*, 2020, 53: 82–90.
- [3] ZHANG An-xin, LI Feng, HUO Peng-da, NIU Wen-tao, GAO Rong-he. Response mechanism of matrix microstructure evolution and mechanical behavior to Mg/Al composite plate by hard-plate accumulative roll bonding [J]. *Journal of Materials Research and Technology*, 2023, 23: 3312–3321.
- [4] TALEBIAN M, ALIZADEH M. Manufacturing Al/steel multilayered composite by accumulative roll bonding and the effects of subsequent annealing on the microstructural and mechanical characteristics [J]. *Materials Science and Engineering A*, 2014, 590: 186–193.
- [5] WANG Zhi-Jie, ZHAI Liang, MA Min, YUAN Hui, LIU Wen-chang. Microstructure, texture and mechanical properties of Al/Al laminated composites fabricated by hot rolling [J]. *Materials Science and Engineering A*, 2015, 644: 194–203.
- [6] LI Xiao-bing, ZU Guo-yin, WANG Ping. Interfacial effect on bending property of Al/Cu/Al laminated composite produced by asymmetrical roll bonding [J]. *Key Engineering*

- Materials, 2014, 575/576: 194–197.
- [7] TANG Jian-wei, CHEN Liang, ZHAN Guo-qun, ZHANG Chun-sheng, SUN Lu. Achieving three-layered Al/Mg/Al sheet via combining porthole die co-extrusion and hot forging [J]. *Journal of Magnesium and Alloys*, 2020, 8(3): 654–666.
- [8] ZHANG Nan, WANG Wen-xing, CAO Xiao-qian, WU Jia-qi. The effect of annealing on the interface microstructure and mechanical characteristics of AZ31B/AA6061 composite plates fabricated by explosive welding [J]. *Materials & Design*, 2015, 65: 1100–1109.
- [9] LUO Chang-zeng, LIANG Wei, LI Xian-rong, YAO Ya-jun. Study on interface characteristics of Al/Mg/Al composite plates fabricated by two-pass hot rolling [J]. *Materials Science Forum*, 2013, 747/748: 346–351.
- [10] ZHANG Xin-ping, YANG Ting-hui, CASTAGNE S, WANG Jing-tao. Microstructure; bonding strength and thickness ratio of Al/Mg/Al alloy laminated composites prepared by hot rolling [J]. *Materials Science and Engineering A*, 2011, 528: 1954–1960.
- [11] LEE Kwang-seok, YOON Dong-hyun, KIM Hye-kyoung, KWON Yong-nam, LEE Young-seon. Effect of annealing on the interface microstructure and mechanical properties of a STS–Al–Mg 3-ply clad sheet [J]. *Materials Science and Engineering A*, 2012, 556: 319–330.
- [12] ZHU Bo, LIANG Wei, LI Xian-rong. Interfacial microstructure, bonding strength and fracture of magnesium–aluminum laminated composite plates fabricated by direct hot pressing [J]. *Materials Science and Engineering A*, 2011, 528: 6584–6588.
- [13] XIA Hong-bo, WANG Shao-gang, BEN Hai-feng. Microstructure and mechanical properties of Ti/Al explosive cladding [J]. *Materials & Design*, 2014, 56: 1014–1019.
- [14] WANG Tao, LI Shao, REN Zhong-kai, HAN Jian-chao, HUANG Qing-xue. A novel approach for preparing Cu/Al laminated composite based on corrugated roll [J]. *Materials Letters*, 2019, 234: 79–82.
- [15] WANG Tao, WANG Yue-lin, BIAN Li-ping, HUANG Qing-xue. Microstructural evolution and mechanical behavior of Mg/Al laminated composite sheet by novel corrugated rolling and flat rolling [J]. *Materials Science and Engineering A*, 2019, 765: 138318.
- [16] YAN Yin-biao, ZHANG Zhong-wu, SHEN Wen, WANG Jin-hua, ZHANG Li-kui, CHIN Ba. Microstructure and properties of magnesium AZ31B–aluminum 7075 explosively welded composite plate [J]. *Materials Science and Engineering A*, 2010, 527: 2241–2245.
- [17] RONG Jian, WANG Peng-yue, ZHA Min, WANG Cheng, XU Xin-yu, WANG Hui-yuan. Development of a novel strength ductile Mg–7Al–5Zn alloy with high superplasticity processed by hard plate rolling (HPR) [J]. *Journal of Alloys and Compounds*, 2018, 738: 246–254.
- [18] HUO Peng-da, LI Feng, WANG Ye, XIAO Xing-mao. Formability and interface structure of Al/Mg/Al composite sheet rolled by hard plate rolling (HPR) [J]. *International Journal of Advanced Manufacturing Technology*, 2022, 118(1/2): 55–65.
- [19] RONG Jian, WANG Peng-Yue, ZHA Min, WANG Cheng, XU Xin-yu, WANG Hui-yuan, JIANG Qi-chuan. Development of a novel strength ductile Mg–7Al–5Zn alloy with high superplasticity processed by hard-plate rolling (HPR) [J]. *Journal of Alloys and Compounds*, 2018, 738: 246–254.
- [20] WANG Tao, GAO Xiang-yu, ZHANG Zhi-xiong, REN Zhong-kai, QI Yan-yang, ZHAO Jing-wei. Interfacial bonding mechanism of Cu/Al composite plate produced by corrugated cold roll bonding [J]. *Rare Metals*, 2021, 40(5): 1284–1293.
- [21] KIM Jung-su, PARK Jaeyeong, LEE Kwang-seok, LEE Sunghak, CHANG Young-won. Correlation between bonding strength and mechanical properties in Mg/Al two-ply clad sheet [J]. *Metals and Materials International*, 2016, 22(5): 771–780.
- [22] HE Bin, CUI Lei, WANG Dong-po, LIU Yong-chang, LIU C X, LI Hui-jun. The metallurgical bonding and high temperature tensile behaviors of 9Cr–1W steel and 316L steel dissimilar joint by friction stir welding [J]. *Journal of Manufacturing Processes*, 2019, 44: 241–251.
- [23] CHANG Hui-hua, ZHENG Ming-yang, XU Cong, FAN Gong-duan, BROKMEIER H G, WU Kai. Microstructure and mechanical properties of the Mg/Al multilayer fabricated by accumulative roll bonding (ARB) at ambient temperature [J]. *Materials Science and Engineering A*, 2012, 543: 249–256.
- [24] LAPOVOK R, NG H P, TOMUS D, ESTRIN Y. Bimetallic copper–aluminium tube by severe plastic deformation [J]. *Scripta Materialia*, 2012, 66(12): 1081–1084.
- [25] LI Sha, LUO Chao, BASHIR M, JIA Yi, HAN Jian-chao, WANG Tao. Interface structures and mechanical properties of corrugated + flat rolled and traditional rolled Mg/Al clad plates [J]. *Rare Metals*, 2021, 40(10): 2947–2955.
- [26] SUHUDDIN U, FISCHER V, dos SANTOS J F. The thermal cycle during the dissimilar friction spot welding of aluminum and magnesium alloy [J]. *Scripta Materialia*, 2013, 68(1): 87–90.
- [27] ZHAO Li-ming, ZHANG Zheng-duo. Effect of Zn alloy interlayer on interface microstructure and strength of diffusion-bonded Mg–Al joints [J]. *Scripta Materialia*, 2008, 58(4): 283–286.
- [28] NIE Hui-hui, HAO Xin-wei, CHEN Hong-sheng, KANG Xiao-ping, WANG Tao-lue, MI Yu-jie, LIANG Wei. Effect of twins and dynamic recrystallization on the microstructures and mechanical properties of Ti/Al/Mg laminates [J]. *Materials & Design*, 2019, 181: 107948.
- [29] USCINOWICZ R. Impact of temperature on shear strength of single lap Al–Cu bimetallic joint [J]. *Composites Part B: Engineering*, 2013, 44(1): 344–356.
- [30] KIM Jung-su, LEE Kwang-seok, KWON Yong-nam, LEE Byeong-joo, CHANG Young-won, LEE Sunghak. Improvement of interfacial bonding strength in roll-bonded Mg/Al clad sheets through annealing and secondary rolling process [J]. *Materials Science and Engineering A*, 2015, 628: 1–10.
- [31] JAMAATI R, TOROGHINEJAD M R. Cold roll bonding bond strengths: Review [J]. *Materials Science and Technology*, 2011, 27(7): 1101–1108.

# 衬板轧制铝/镁/铝复合板的波纹界面结构及形成机理

霍鹏达<sup>1</sup>, 李峰<sup>1,2,3</sup>, 王野<sup>1</sup>, 李超<sup>1</sup>

1. 哈尔滨理工大学 材料科学与化学工程学院, 哈尔滨 150040;
2. 哈尔滨理工大学 先进制造智能技术教育部重点实验室, 哈尔滨 150080;
3. 哈尔滨工业大学 微系统与微结构制造教育部重点实验室, 哈尔滨 150001

**摘要:** 提出一种采用衬板轧制进行 AA1060 铝/AZ31B 镁/AA1060 铝复合板的制备方法。结果表明: 传统轧制铝/镁/铝复合板截面轮廓较为平直, 而衬板轧制由于衬板可将剪切力部分转化为压应力, 从而改变复合板受力状态, 在铝/镁界面连接处形成差速流动, 故而界面轮廓呈现波浪状特征, 层间实现互锁连接。界面连接强度为 64 MPa, 是传统轧制复合板的 4 倍。力学性能测试表明: 衬板轧制复合板的抗拉强度可达 210 MPa, 比传统轧制法提高 12.3%。综上可知, 衬板轧制法为高性能铝/镁/铝异质复合板成形制造提供一种新思路。

**关键词:** 衬板轧制; 铝/镁/铝复合板; 界面形貌; 连接强度; 力学性能

(Edited by Bing YANG)